The Intrigues and Delights of Kleinian and Quasi-Fuchsian Limit Sets

CHRIS KING

Introduction: My research in dynamical systems has inexorably led me from the better-known fractal dynamics of Julia and Mandelbrot sets, including those of the Riemann Zeta function[1], to the more elusive forms of Kleinian limit sets.

Julia sets and their universal atlases, Mandelbrot sets, have become ubiquitous features of the mathematical imagination, demonstrating the power of computer algorithms to generate, in scintillating detail, visualizations of complex dynamical systems, complementing theory with vivid counter-examples. However Gaston Julia's original explorations took place abstractly, long before the explosion of computing technology, so it was impossible to appreciate their fractal forms and it was only after Beniot Mandelbrot popularized the set that now bears his name that the significance of Julia's work again became recognized. It is a historical irony, very pertinent to this article, that the Mandelbrot set was actually discovered by Robert Brooks and Peter Matelski[2] as part of a study of Kleinian groups. It was only because Mandelbrot was a fellow at IBM that he had the computing resources to depict the set in high resolution, as a universal multi-fractal atlas.

Julia sets and are generated by iterating a complex polynomial, rational or other analytic function, such as exponential and harmonic functions. For a non-linear function, exemplified by the quadratic iteration $z \to f_c(z) = z^2 + c$, successive iterations either follow an ordered pattern, tending to a point, or periodic attractor, or in a complementary set of cases, behave chaotically, displaying the butterfly effect and other features of classical chaos. The Julia set is the set of complex values on which the iteration is chaotic and the complementary set, where it is ordered, is named after the Julia set's co-discoverer Pierre Fatou. The Mandelbrot set *M*, fig 1(h), becomes an atlas of all the Julia sets J_c, by starting from the critical point: $z_0 : f'(z_0) = 0$ (the last point to escape to infinity) and applying the iteration for every complex *c*-value. In a fascinating demonstration of algorithmic topology, if $c \in M$ the fractal Julia set J_c of *c* is topologically connected, otherwise J_c forms a totally-disconnected fractal dust, or Cantor set, with the most ornate and challenging examples lying close to, or on, the boundary of *M*.

Alongside images on the internet of complex fractals, you will also find a more esoteric class of fractal sets that often look like medieval arboreal tapestries, and go variously by the names of Kleinian and quasi-Fuchsian limit sets, but the programs that generate them are much more difficult to find – to such an extent that I resolved to generate accessible multi-platform versions in the public domain to enable anyone to explore them.

To make these fascinating systems freely accessible and to aid further research, I have thus developed an interactive website: [Kleinian and Quasi-Fuchsian Limit Sets: An Open Source Toolbox](), [3] with freely available cross-platform software, including a Matlab toolbox and a generic C script, a hundred times faster, that will compile and generate images on any GCC-compatible operating system, as well as a MacOS viewing app, enabling full dynamical exploration of the limit sets at will. These limit sets also have an intriguing history, which I will sketch only briefly, as it is elucidated in definitive and engaging detail in **Indra's Pearls: The Vision of Felix Klein**[4]. Interspersed below are short references (e.g. ***IP1***) so one can refer to an expanded discussion of each topic by browsing the book.

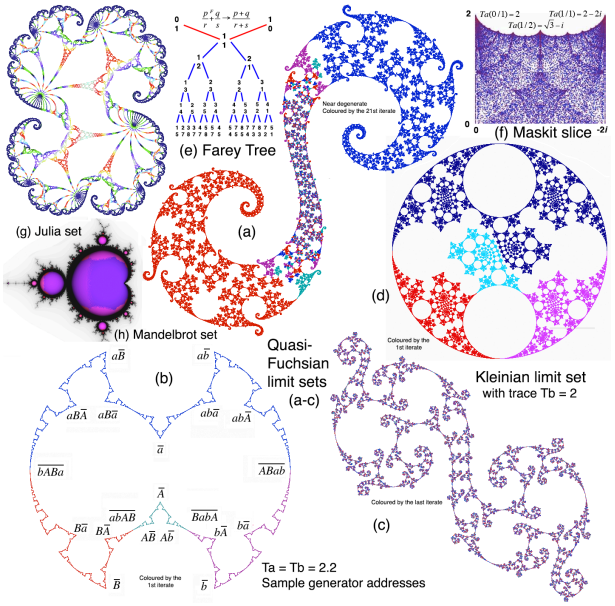

Fig 1: Julia sets and Kleinian limit sets (a-c) are two classes of complex fractals, the former being the set on which a non-linear function, is chaotic, and the latter the limit set of two interacting Möbius transformations. Just as Julia sets (g) have the Mandelbrot set (h), as atlas, limit sets with T*b*=2, as in fig 3 have the Maskit slice (f) as atlas, with the critical states on the upper boundary.

In this field, we again witness an evolution, where research and discovery has at first been driven by abstract theoretical advances, which are then

followed by the emergence of innovative computational approaches that yield critical examples displaying the richness and variety that gives the theory its full validation.

The field of Kleinian groups was founded by Felix Klein and Henri Poincaré, the special case of Schottky groups having been elucidated a few years earlier by Friedrich Schottky. The ensuing story, as depicted in Indra's Pearls begins with a visit to Harvard by Benoit Mandelbrot that leads to David Mumford setting up a computational laboratory to explore "some suggestive 19th century figures of reflected circles which had fascinated Felix Klein". Caroline Series along with David Wright, assisted by Curt Mullen who had held summer positions at IBM, and other collaborators such as Linda Keen, then began to investigate computational exploration of these limit sets. In David Wright's words: "Take two very simple transformations of the plane and apply all possible combinations of these transformations to a point in the plane. What does the resulting collection of points look like?" Indra's Pearls continues this human and mathematical journey in elegant detail, noting the contributions of many researchers, including Bernard Maskit and Troels Jørgensen to the unfolding exploration of the area.

A Mathematical Nexus: By contrast with Julia sets, Kleinian limit sets are algebraic 'attractors' generated by the interaction of two Möbius maps *a, b* and their inverses $A = a^{-1}$, $B = b^{-1}$. Möbius maps ***IP62*** are fractional linear transformations operating on the Riemann sphere $\mathcal{R}$, fig 2(a), represented by complex matrices. Composition of maps is thus equivalent to matrix multiplication:

$$z \to a(z) = \frac{pz+q}{rz+s} \approx \begin{bmatrix} p & q \\ r & s \end{bmatrix} \begin{bmatrix} z \\ 1 \end{bmatrix} : ps - qr = 1 \ (1).$$

Möbius transformations can be elliptic, parabolic, hyperbolic, or loxodromic[a], in terms of their trace $Tr(a) = p + s$, as complex generalizations of the translations, rotations and scalings of affine maps of the Euclidean plane. They map circles to circles on $\mathcal{R}$, counting lines in the complex plane as circles on $\mathcal{R}$. Möbius maps are thus simpler in nature than analytic functions and are linear and invertible, so a single Mobius map will not generate an interesting fractal. However, when two or more Möbius maps interact, the iterations of points in $\mathcal{R}$, under the two transformations and their inverses, tend asymptotically towards a set which is conserved under the transformations, often a complex fractal, called the **limit set** of the group. When the two transformations acting together form certain classes of group, including Kleinian, quasi-Fuchsian and Schottky groups, their limit sets adopt forms with intriguing mathematical properties.

Because they form an interface between widely different mathematical areas, their dynamics draw together diverse fields, from group theory, through topology, Riemann surfaces and hyperbolic geometry, to chaos and fractal analysis, perhaps more so than any related area. Depending on the particular group, its action[b] may transform the topology of the Riemann sphere into that of another kind of topological surface, such as a two-handled torus, sometimes with pinched handles, fig 2 (e-g).

A Kleinian group is a discrete[c] subgroup of 2 x 2 complex matrices of determinant 1 modulo its center - the set of elements that commute with every element of the group.

A Schottky group ***IP96*** is a special form of Kleinian group, consisting of two (or more) of Möbius maps *a* and *b* on $\mathcal{R}$, each of which maps the inside of one circle *C* onto the outside of the other *D*. If the two pairs of circles are entirely disjoint as in fig 2(b), the group action induces a topological transformation of $\mathcal{R}$, generating a multi-handled torus as in fig 2(e).

A quasi-Fuchsian group ***IP161*** is a Kleinian group whose limit set is contained in an invariant Jordan curve, or topological circle, so their limit sets are fractal circles. The underlying spaces of quasi-Fuchsian and other Kleinian groups, such as that of the Apollonian gasket fig 2(d), can be defined by pinching the topology as in (f, g), so that the limit set becomes a fractal tiling by circles as in fig 3(a).

The group interactions, when discrete, induce tilings in the complex plane, which also illustrate transformations of hyperbolic geometry[d].

---

[a] **Parabolic** maps have $Tr^2(a)=4$ and act like translations, with one fixed point on $\mathcal{R}$, **elliptic** maps have $0<Tr^2(a)<4$ and behave like rotations on $\mathcal{R}$, **hyperbolic** and **loxodromic** maps have real and complex values lying outside these values on $\mathcal{C}$ and behave like (spirally) expanding and contracting versions of scalings on $\mathcal{R}$.

[b] This new topology arises from the quotient of the complement of the limit set under the action of the group.

[c] A **discrete** group is a group of transformations of an underlying space possessing the discrete topology, where there is a collection of open sets in which each open set corresponds to just one element of the group. Discrete groups thus appear naturally as the symmetries of discrete structures, such as tilings of a space.

[d] The group of all Möbius transformations is isomorphic to the orientation-preserving isometries of hyperbolic 3-space $\mathcal{H}_3$, in the sense that every orientation-preserving isometry of $\mathcal{H}_3$ gives rise to a Möbius transformation on $\mathcal{R}$ and vice versa. Hence group actions of such transformations can generate hyperbolic tilings. Maurice Escher's "Angels and Demons" tiling is a representation of the modular group, which is also manifest in the

As the parameters of these maps vary, the limit sets approach a boundary in parameter space, where the limit set can become a rational circle packing, as in fig 3(a-c) or irrationally degenerate (f, g), forming a space-filing fractal, beyond which the process descends into chaotic dynamics fig 6(d), as the groups become non-discrete and their orbits become entangled. Like the Mandelbrot set, for certain classes of limit set, one can generate an atlas, called the Maskit slice, fig 1(f), whose upper boundary contains these limiting cases.

An insightful way to portray their actions is to determine what the Möbius transformations do to key circles involved in the definitions of *a* and *b*. A good starting point is with pairs of Schottky maps. If all the circles are disjoint, when the circles are transformed by both maps, their images form a cascade of circles, which tend in limit to a Cantor set, fig 2(b). As the parameters *p*, *q*, *r*, and *s* of each are varied, so that circle pairs come together and touch, as in (c), the Cantor set transforms into a circular limit set.

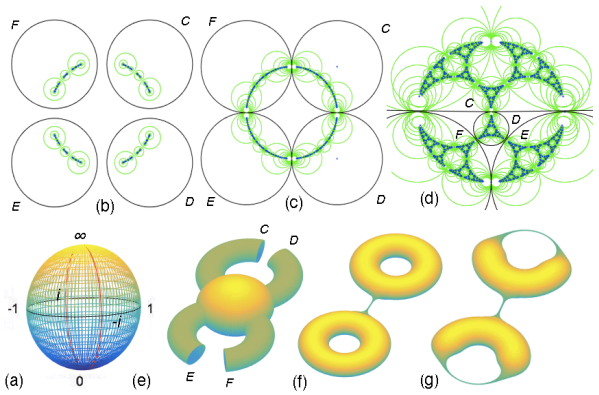

Fig 2: (a) The Riemann sphere – the complex plane closed by a single point at infinity. (b) Schottky maps forming Cantor dust. (c) Touching circles forming a circular limit set. (d, g) Four circles, all touching, forming an Apollonian gasket. (e) Schottky maps perform a surgery of $\mathcal{R}$ to form a double handled torus. (f) If the commutator is parabolic, as in quasi-Fuchsian limit sets, which form a fractal topological circle, or Jordan curve, whose complements, quotient by the group into a pair of Riemann surfaces, the double torus becomes pinched. (g) When one or both of *a* and *b*, or their words, are also parabolic, as in the gasket, (d) and those in fig 3, one, or two further pinches occur.

There is an alternative way, independently of Schottky groups, to uniquely define the matrices via their traces T*a*, T*b*, where T*a* = *p* + *s*, as in (1), if we focus on maps where the commutator $aba^{-1}b^{-1}$ is parabolic, with T($aba^{-1}b^{-1}$) = –2, inducing a cancellation in (2) below. Since traces are preserved under conjugacy of mappings $b = cac^{-1}$, we can simplify the discussion to conjugacy classes, reducing the number of free variables in the two matrices to a unique solution. This, process, affectionately known in Indra's Pearls as 'Grandma's recipe' ***IP227***, enables us to explore new classes of limit set, as illustrated in fig 2(d) for the Apollonian gasket, which can also be represented via 4 circles, all of which touch, as shown in black.

The asymmetric nature of the two matrix mappings generated by Grandma's recipe can be seen in fig 1(b, d), where both are coloured by the first iterate. Although the commutator is parabolic (resulting in the single pinch we see in fig 2(f), the generators *a*, and *b* can be loxodromic, and can tend to parabolic as well, with the transition from the quasi-Fuchsian set of fig 1(b) where T*a* = T*b* = 2.2 to the Apollonian gasket fig 3(a), where T*a* = T*b* = 2, resulting in the two further pinches in fig 2(g) and in each of the examples in fig 3, where *b* is parabolic with T*b* = 2.

Because the limit set is the place where all points are asymptotically mapped under interaction of the transformations and their inverses, one can simply pick each point on the plane and repeatedly map it by a random sequence of the two transformations and their inverses and these points will become asymptotically drawn to the limit set. The trouble with this process is that, although it can crudely portray any limit set, including chaotic, non-discrete examples, the asymptotic iterates are distributed exponentially unevenly, so that some parts of the limit set are virtually never visited and the limit set is incompletely and only very approximately portrayed, as in fig 6(d).

By contrast with the non-linear functions of Julia sets, where depiction algorithms, such as modified inverse iteration fig 1(g) and distance estimation, depend on analytic features, such as derivatives and potential functions, an accurate description of Kleinian group limit sets requires taking full strategic advantage of the underlying algebraic properties of the group transformations.

Descending the Spiral Labyrinth: The depth-first search algorithm ***IP141*** to depict the limit sets is ingenious and extremely elegant. The aim is to traverse the algebraic space of all word combinations of the generators a, *b*, a^{-1}, b^{-1} in a way which draws a continuous piecewise linear approximation to the fractal of any desired resolution.

To do this, we generate a corkscrew maze, where we traverse deeper and deeper layers of the search tree, turning right at each descent and then enter each tunnel successively, moving anticlockwise around the generators, and retreating when we reach the inverse of the map we entered by, after three left turns, since the map and its inverse cancel. At each node we retain a record of our journey down, our Ariadne's thread, by multiplying the successive matrices as we descend, and make a critical test: The parabolic commutator has a single fixed point, which represents an infinite limit of cyclic repeats of the

---

symmetries of the gray Apollonian gasket discs ***IP206***, in fig 3(a), and has a similar topological pinching ***IP216*** to fig 2(g).

generators. If we apply the composed orbit matrix to the fixed point of the clockwise commutator and do the same for the anti-clockwise commutator's fixed point and these two are within an epsilon threshold, this means going the 'opposite way' around the local fractal leaves us within resolution, so we draw a line between the two and terminate the descent, retreating and turning into vacant tunnels and exploring them, until we find ourselves back at the root of the tree.

Using the fixed points has the effect of producing a theoretically infinite orbit of transformations that can carry us to any part of the limit set, and because we are traversing generator space systematically, we will traverse parts of the limit set that are visited exponentially rarely in a random process.

Navigating the Maskit Slice: If we focus on limit sets where b is parabolic with Tb = 2, and only Ta varies, this gives us a complex parameter plane called the Maskit slice ***IP287***, fig 1(f), forming an atlas of limit sets, just as the Mandelbrot set does for Julia sets, so we can explore and classify their properties. To define locations on the slice, we need to be able to determine the traces Ta that correspond to rational cases involving fractional motion. Key to this are the generator words formed by the maps. For example 3/10 in fig 3(c) has a parabolic generator word $a^3Ba^4Ba^3B$ symbolically expressing the 3/10 ratio, which I also parabolic. For general fractional values p/r we can determine the traces recursively from two key relations – extended Markov and Grandfather ***IP192***:

$$\mathrm{T}aba^{-1}b^{-1} = \mathrm{T}^2a+\mathrm{T}^2B+\mathrm{T}^2aB - \mathrm{T}a.\mathrm{T}B.\mathrm{T}aB - 2 \quad (2)$$

$$\mathrm{T}mn = \mathrm{T}m.\mathrm{T}n - \mathrm{T}m^{-1}n \quad (3).$$

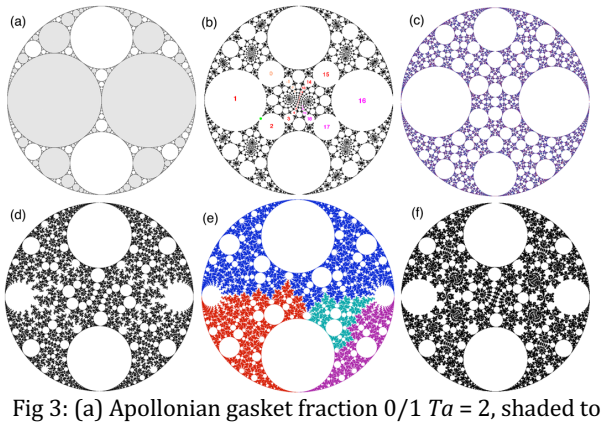

Fig 3: (a) Apollonian gasket fraction 0/1 Ta = 2, shaded to highlight separate components in the mapping, (b) the 1/15 limit set with the 15 steps of the parabolic word $a^{15}B$ in red. Intriguingly, as $1/n$ –> $1/\infty = 0$, the limit sets do not tend to the gasket, although their traces and matrices do, as the limiting limit set has an additional fourfold symmetry of rotation by $\pi/2$ already evident in (b). (c) The 3/10 set coloured by the last iterate. (d) A free discrete group. (e) Singly-degenerate Farey $(LR)^\infty$ set of the Golden mean. (f) Spirally degenerate $(L^{10}R)^\infty$ set.

We can use these relations to successively move down the Farey tree of fractions ***IP291***, see fig 1(e), because neighbours on the tree have generator words combining via Farey mediants $w_{p+q/r+s} = w_{p/r}w_{q/s}$, and so the grandfather identity implies $Tw_{p+q/r+s} = Tw_{p/r}\,Tw_{q/s} - Tw_{p-q/r-s}$ because, in the last term, the combined word $m^{-1}n$ has neatly cancelling generators in the middle. Since $\mathrm{T}aba^{-1}b^{-1} = -2$ in (2), for p/r, this reduces to solving an r-th degree polynomial.

If we plot all the polynomial solutions to the p/r limit sets, for $r \le n$ we have the Maskit slice ***IP287***, fig 1(f), whose upper boundary contains each of the p/r trace values as fractal cusps. Above and on the boundary are discrete groups, which generate fractal tilings of the complement in $\mathcal{R}$, while values within the slice produce non-free groups or chaotic non-discrete sets, which can generally be portrayed stochastically, fig 6(d), but not by depth-first search.

The rational cusps ***IP273*** provide intriguing examples of circle packings with deep links to hyperbolic geometry. However, irrationally degenerate space-filling limit sets remained enigmatic, until a key example trace value was found ***IP314***, named after Troels Jørgensen, who posited the existence of such limit sets[5]. The solution is completely natural – the Golden mean limit of the Fibonacci fractions arising from a repeated LR move on the Farey tree resulting in the limit set of fig 3(e). We can approach such values by use of Newton's method to solve the equations of the ascending fractions.

This leads on to further cases, such as spiral degeneracy ***IP320***, where we repeat a ten to one set of moves, $L^{10}R$, up the left hand slope of the Maskit slice upper boundary, and into a spiraling sequence of ever smaller cusps in the slice, giving rise to the limit set of fig 3(f). Since irrational numbers are uncountable, such limit sets are the overwhelming majority of cases, although harder to access.

Double degeneracy at the Edge of Chaos: The above examples are singly degenerate, because only half the region is engulfed, and the question arises, is it possible to find a pair of traces generating a limit set which is entirely space-filling, permeating the complex plane with a fractal dimension of 2? This quest became a mathematical epiphany ***IP331***. It is possible to generate a limit set conjugate to Troels' example in the following way. To make a LR journey down the Farey tree to a higher Fibonacci fraction, such as 987/1597, about the middle, we find 21/34 and 13/21. It turns out that the words in terms of a and B for these steps also form generators which can be used in reverse to define a and B. If we apply Grandma's algorithm to their traces calculated by matrix multiplication of the a and B words, we get another limit set conjugate to the original, as in fig 4(a).

The reasoning that these two midpoint traces were very similar led to the idea that a doubly degenerate limit set corresponding to the Golden mean might

arise from simply applying endless LR Farey moves $(a,B)\overset{L}{\rightarrow}(a,aB)\overset{R}{\rightarrow}(a^2B,aB)$, which leave the generators unchanged: $(a, B) = (a^2B, aB)$, giving two equations which, combined with Grandfather and Markov leads to the conjugate trace solutions $(3 \pm 3^{1/2}\, i)/2$, as shown in fig 4(b).

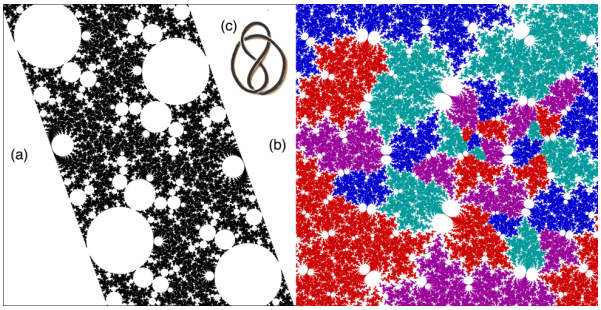

Fig 4: (a) Limit set conjugate to the Golden mean limit set. (b) The doubly degenerate space-filling limit set of fractal dimension 2, coloured by the third iterate to highlight the fractal line connecting centres. (c) Figure 8 knot, whose 3D complement is glued from hyperbolic 3-space by (b).

An intriguing feature is that, in addition to *a*, *b*, there is a third induced parabolic symmetry *c*, because the (LR)∞ move must arise from a Möbius map conjugating the limit set to itself, which has the same fixed point as the parabolic commutator, and conjugates with it, although performing a distinct 'translation' flipping the sets bounding the jagged line connecting the centres. Robert Riley[6] has shown that the 3 transformations result in a gluing of 3D hyperbolic space, via the group's discrete 3D 'tiling', to become the 3-sphere with the figure 8 knot (fig 4 inset) removed ***IP388***.

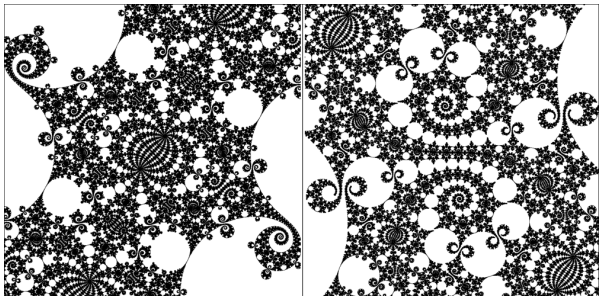

Fig 5: The 'Holy Grail' – double spiral degeneracy, with the traces reversed in the second image. The convergence to space-filling is very slow and the full resolution image took 29 hours in generic C and would have taken 112 days in interpreted Matlab code. Although the traces are no longer conjugates, the sets are clearly degenerate on both complement components in the same way as in fig 4.

To unravel the spirally degenerate case, I examined the recursive relations from the endless $(L^{10}R)^{\infty}$ move and found they could be exploited to produce a pair of traces by solving a system of 11 equations: T*a* = 1.936872603726 + 0.021074052017*i*, and T*b* = 1.878060670271 – 1.955723310188*i*. When these are input into the DFS algorithm, we have the double spiral degeneracy shown in fig 5.

The Bondage of Relationships: There is a further enchanting collection of limit sets ***IP353***, where the group is non–free and has an elliptic commutator that powers to the identity – $(aba^{-1}b^{-1})^n = I$. For n=2, this causes the trace to be 0, but an extended grandma's algorithm ***IP261*** applies, so the recursive relations (2) and (3) can be solved to give a polynomial, and the limit sets can be depicted by DFS, as long as generator words that short-circuit to the identity are treated as dead-ends.

This requires an automatic group – involving a Finite State Automaton, or FSA – a look-up table, where all the growing word strings that could end in a short-circuit, as we descend the search tree, are accounted, by iteratively composing their states and exiting when a death state is reached. In fig 6(a-c), are three such limit sets, with the "inner" regions highlighted in yellow to distinguish them from the complementary white regions, from which they are isolated by the limit set. For varying elliptic commutators a utility called MAF[7] can generate such FSAs by inputting the relations e.g. *a*^3=I, *abAB*^7=I.

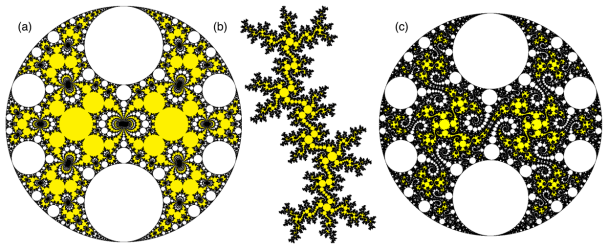

Fig 6: Non-free limit sets, (a) T*a*(1/60) T*b*=2 , (b) a quasi-Fuchsian "dragon" (c) $L^{10}R$ spirally degenerate.

Islands on the Elliptic Shoreline:

The advent of elliptic commutators, whose powers of *n* become the identity, combined with elliptic generators means the quasi-circular form of the limit set gives way to fractal islands displaying the underlying form of a hyperbolic space. There is a natural way of making a normalisation of the limit set, displaying the intrinsic symmetry of the commutator around a central motif generated by the Möbius maps represented by *a* and *b*. This is called the symmetric-inverse normalization.

In this situation, FSAs can be streamlined to find the exact symmetries in MAF, by using an additional involution *x*: $x^2 = -I$ so that $xax = -a^{-1}$, $xbx = -b^{-1}$ and $-(abx)^2 = aba^{-1}b^{-1}$ becomes the "square root" of the commutator, defining the underlying symmetries.

For example, the left hand limit set in fig 7 is generated by picking a loxodromic *a*, a complementary *b* such that $(ab)^3 = I$ and commutator square root $(abx)^7 = I$. The resulting FSA can then be translated back to the *a*, *b*, a^{-1}, b^{-1} form to depict the limit set.

The symmetric inverse normalization can easily be derived from the grandma normalization by transforming a and b to $e = a^{-1}b^{-1}$ and $f = a^{-1}$ and conjugating the result with c = [1 1;-1 1] to get generators cec^{-1} and cfc^{-1}.

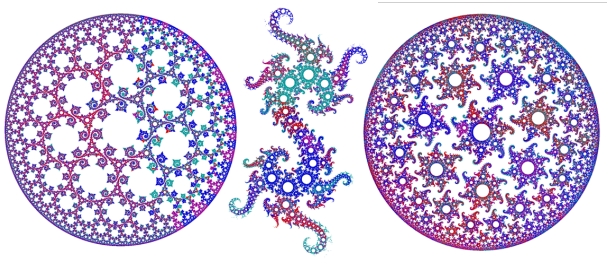

Fig 7: Left: a loxodromic, $(ab)^3$= I, $(axb)^7$ = I. Right: a loxodromic, $(ab)^7$= I, $(axb)^7$ = I in symmetric inverse normalization. Centre: The right hand set in grandma normalisation has a wild loxodromic boundary, because the generators a and b are both loxodromic, although co-related by elliptic $(ab)^7$= I. Sets coloured by iterate.

If we go one step further and assign all three traces to be elliptic, we arrive at a situation where there is only a single limit set defined for each set of three symmetries.

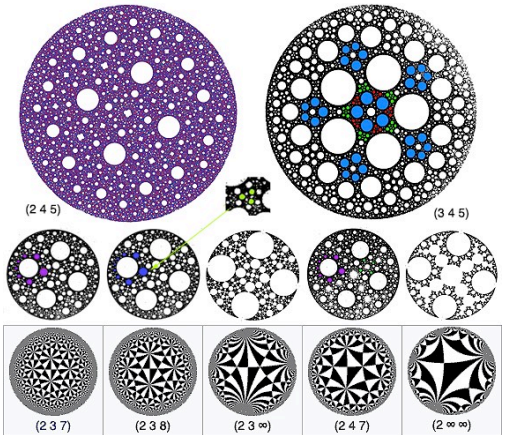

Fig 8: Examples of limit sets where there are three elliptic traces , showing top left and lower rows, limit sets corresponding to triangle group tilings in the hyperbolic plane and top right limit set where T$\underline{a}$, Tb and T$abAB$ have 3, 4, and 5-fold symmetries, highlighted in red, green and blue. Top left has $(ab)^5$=I $(aB)^4$=I and abAB is a rotation by π, so that $(abAB)^2$=I. Symmetries in the middle row are also highlighted in colour. The top left set is by depth first search and the others are generated using the stochastic algorithm below.

Falling into the Chaotic Abyss: Using the stochastic algorithm, one can also freely explore the wilder limit sets. This recursively maps chosen points, such as Möbius transformation fixed points, using a random sequence of the four generators. This can visualize limit sets in lower fidelity without any restriction, including non-free, and non-discrete chaotic systems, as illustrated in fig 9.

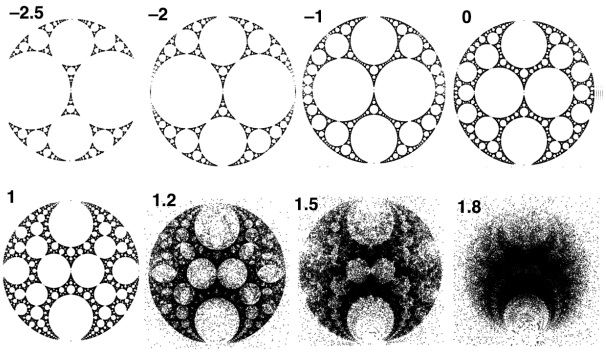

Fig 9: A succession of non-free and non-discrete chaotic limit sets where Ta = Tb = 2 under a varying commutator trace, using the stochastic algorithm.

References:

[1] Chris King 2011 *Fractal Geography of the Riemann Zeta Function* arXiv:1103.5274.

[2] Robert Brooks and Peter Matelski, *The dynamics of 2-generator subgroups of PSL(2,C)*, in Irwin Kra, ed. 1981 Riemann Surfaces and Related Topics: Proceedings of the 1978 Stony Brook Conference, Princeton University.

[3] Chris King 2018 *Kleinian and Quasi-Fuchsian Limit Sets: An Open Source Toolbox* http://dhushara.com/quasi/

[4] David Mumford, Caroline Series and David Wright 2002 **Indra's Pearls: The Vision of Felix Klein** Cambridge ISBN 978-0-521-35253-6.

[5] Troels Jorgensen 1977 *Compact 3-Manifolds of Constant Negative Curvature Fibering Over the Circle* Ann. Math. Ser 2, 106(1) 61-72.

[6] Robert Riley 2013 *A personal account of the discovery of hyperbolic structures on some knot complements* Expo. Math. 31 104-115 doi:10.1016/j.exmath.2013.01.003.

[7] Williams Alun *Monoid Automata Factory* http://maffsa.sourceforge.net/